

Models for contact-mediated pattern formation: cells that form parallel arrays

Leah Edelstein-Keshet¹ and G. Bard Ermentrout²

¹ Mathematics Department, University of British Columbia, Vancouver, BC, Canada V6T 1Y4

² Mathematics Department, University of Pittsburgh, Pittsburgh, PA 15260, USA

Received July 18, 1989; received in revised form January 8, 1990

Abstract. Kinetic continuum models are derived for cells that crawl over a 2D substrate, undergo random reorientation, and turn in response to contact with a neighbor. The integro-partial differential equations account for changes in the distribution of orientations in the population. It is found that behavior depends on parameters such as total mass, random motility, adherence, and sloughing rates, as well as on broad aspects of the contact response. Linear stability analysis, and numerical, and cellular automata simulations reveal that as parameters are varied, a bifurcation leads to loss of stability of a uniform (isotropic) steady state, in favor of an (anisotropic) patterned state in which cells are aligned in parallel arrays.

Key words: Cell motion – Contact response – Pattern formation – Cell alignment – Parallel arrays – Biological cellular automata – Integro-partial differential equation models

1. Introduction

Pattern formation and self-organization are population phenomena that transcend properties of individuals, and yet are ultimately explained by interactions of individuals with their environment or with each other. Cellular biology provides a rich variety of examples of pattern forming mechanisms including: (a) the guidance of cells by predetermined chemical gradients (chemotaxis), (b) guidance by physical cues such as fibers, (c) differential adhesivities of cells to each other or to the environment (haptotaxis), and (d) mechanical stresses that lead to motion along the path of least resistance (Keller and Segel 1970; Murray and Oster 1984; Oster et al. 1983; Harris et al. 1984; Stopak and Harris 1982). However, relatively few cases of pattern formation outside the realm of neurobiology have been attributed to direct cell-cell interactions, without chemical gradients, mechanical stresses or long-range communication of some sort. In this paper, we consider an example in which cell-cell interactions alone produce pattern or structure.

The example analyzed here stems from a biological observation due to Elsdale (1972, 1973), who found that a collection of cells initially oriented at

random has the tendency to align and form parallel arrays. Elsdale's observations were made on cultures of fibroblasts—cells which crawl on a surface, exhibit contact responses, and are known to use a variety of guidance cues in navigating. (See Stopak and Harris 1982.) However, even in absence of such cues (e.g., in collagen-free cultures) the alignment phenomenon persisted.

Similar, or related, phenomena apparently occur in many systems, both macroscopic and microscopic, biological and physical. Alignment can be seen in members of a herd or flock, in tissues such as insect cuticle epidermal cells (Nübler-Jung 1987), in colonies of swarming microorganisms (see, for example, the recent review by Shapiro 1988), and even in the physical setting of liquid crystals (e.g. see Priestly et al. 1974). The mechanisms clearly differ, although certain common features are present.

The purpose of this paper is to determine whether Elsdale's observations can be explained from contact-responses of the cells alone. We do not imply or suggest that guidance cues, whether chemical or mechanical are not important influences—on the contrary, their importance has been clearly established in the literature cited above. Rather, we view our model as a mathematical thought-experiment in which all influences other than the minimal fibroblast behavior have been stripped away. Our aim is to expose aspects of collective behavior that *could* be accounted for at this level.

We proceed from experimental cell-contact response data due to Erickson (1978) and formulate a set of equations to describe collective behavior. As an end result we find that, under appropriate conditions—namely when the density of the cells has reached a critical level—a spontaneous tendency to align along some common axis of orientation occurs. Thus, the individual behavior of cells as well as their tendency to adhere in clumps proves to be sufficient to account for the phenomena that Elsdale observed. External gradients, mechanochemical factors, stress lines in the extracellular milieu, or contact guidance by fibers or oriented macromolecules would then be competing influences that either enhance this phenomenon, or override it. The prediction that structure or pattern can arise from cellular contact responses alone forms the centerpiece and the chief new result of our paper.

The organization of this paper is as follows: in Sects. 2 and 3, we describe the biological background and mathematical preparation for the models. Section 4 sets out the strategy for the sequence of models described in Sects. 5 and 6, and Sect. 7 presents results of cellular-automation simulations. Finally, we close with some general discussion and applications to other systems in Sect. 8.

2. Fibroblast biology

Fibroblasts are cells which are found in connective tissue, and which play a role in wound-healing. They can be isolated from a variety of sources (including fetal connective tissue, skin, salivary gland, mammary gland, and kidney), retain many of their properties *in vitro* and can be studied in a two-dimensional system less complicated than that of their natural environment (but see also Bard and Hay 1975). Individual cells placed in a Petri plate will attach to the substrate and crawl. Locomotion is achieved by the extension of a leading edge (called the lamellipodium, or ruffled membrane) which moves forward, adheres to the substratum, and pulls the cell. Breaking of adhesion in the rear causes the cell to advance (Lackie 1986). The lamellipodium resembles protruding webbed

“fingers” or ruffles that appear to “feel” the environment. Net motion derives from competing pulls of many ruffles on the lamellipodium. For this reason, the cell occasionally veers off from its previous direction of motion and reorients, so that motion consists of straight paths interspersed with occasional turns.

When a portion of the lamellipodium comes into contact with another cell, it freezes momentarily and retracts. This is contact inhibition of motion (CIM) and is surface-specific. According to Erickson (1978), when a pair of cells come into contact at a small angle, only a fraction of the lamellipodium is inhibited, and the contacting cell glides along its neighbor, realigns, and adheres to it. At larger angles of contact, (beyond some angle $\varphi = a$), cells may crawl over or under one another without realigning. The dependence of the outcome on the angle of contact is documented by Erickson (1978) and Elsdale (1973), who find that the critical angle, a , is species-dependent. For example, $a = 20^\circ$ for human fetal lung fibroblasts (HFL) (Elsdale 1973) and $a = 55^\circ$ for baby hamster kidney cells (BHK) (Erickson 1978).

Elsdale (1973) grew fibroblasts under conditions which prevent the formation of collagen, a substance which fibroblasts normally secrete and which then provides landmarks and trails that cells follow. He observed that initially the cells are free and move independently. However, clusters of parallel cells start to form. In such clusters, cells maintain motion along the axis of the cluster but cannot readily reorient due to contact inhibition by neighbors. Through recruitment and loss of cells, such clumps grow or diminish in size until a two-dimensional mosaic of patches, called *parallel arrays* is created (see Fig. 1). Typically, a patch consists of hundreds of cells in a single-cell-thick layer with a given axis of orientation. There is a tug-and-pull competition between contiguous patches so that if the process is allowed to continue, eventually a single array with one axis emerges.

In this paper we ask several questions about the formation of parallel arrays. First, we ask what type of cellular interactions can account for the observation that cells form parallel arrays. Second we ask what determines the predominant orientation of such an array. Finally, we consider how details of the biology affect aspects of the patterns formed. Our thesis is that the selection of a preferred axis of orientation stems from the fact that the uniform steady state (one in which cells are uniformly distributed in orientation) is unstable. We use linear stability theory to test for the presence of such instability, and numerical methods for studying the dynamics.

3. Mathematical preparation

In deriving equations for the population of cells we proceed from the behavior at the individual cell level. The repertoire of a single cell consists of (a) persistence in the direction of motion, (b) sporadic random turns, (c) turns and adherence upon contact with another cell. We assume that the probability of a random turn by angle φ per unit time is $\alpha(\varphi)$, and that clockwise or anticlockwise turns are equally probable: $\alpha(\varphi) = \alpha(-\varphi)$. We define $K(\varphi)$ to be the probability that a cell contacting a neighbor at relative angle φ aligns with it and sticks. The nature of K , discussed further below, is deduced from experimental data.

At the population level it is possible to formulate a set of equations which would describe both the spatial distribution of cells and their orientations. For

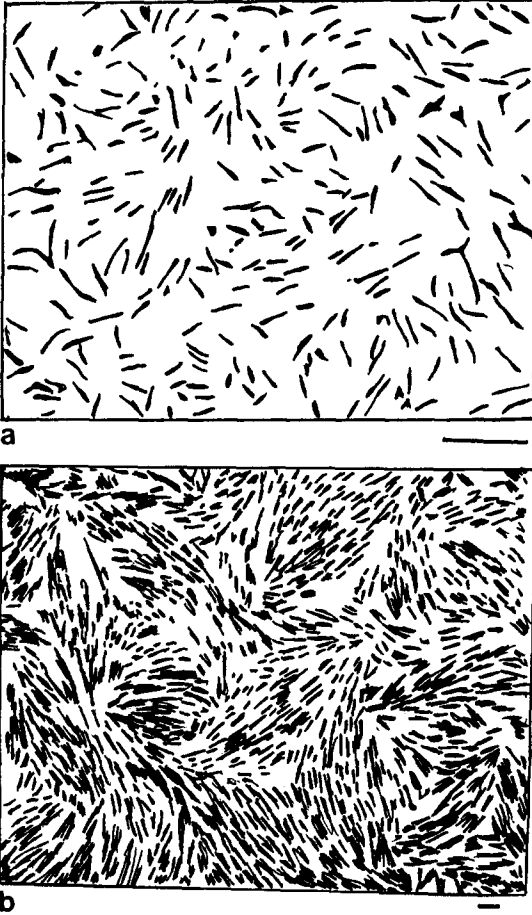


Fig. 1a,b. Artificially grown cultures of fibroblasts showing two stages of development. **a.** Initial configuration: free cells move, crawl, reorient randomly, and proliferate. **b** Later stages: a dense population in which cells are organized into parallel arrays. Cells are free to move along the axis of an array but cannot reorient because neighboring cells exert contact inhibition of motion. *Bar scales: a* 1000 μ ; *b* 100 μ . *Sketched following Elsdale (1973)*

example, $C(x, \theta, t)$ might be defined as density of cells at x moving in direction θ , and $v = v(\cos \theta, \sin \theta)$ their velocity vector. However the resulting model is quite difficult to understand analytically. Since our main focus is the orientation of cells, we here consider only angular distributions of cells, not spatial distributions. Thus, cell densities are functions of time and of θ , the angle of orientation: $C(\theta, t)$ is the density of cells whose orientation (with respect to some fixed direction) is θ at time t . θ is an angle, $(-\pi \leq \theta \leq \pi)$ and all functions of θ , including C are assumed to be periodic ($C(-\pi, t) = C(\pi, t) \forall t$).

Fixing attention on some arbitrary angle θ , we observe that with probability $\alpha(\varphi) = \alpha(-\varphi)$ $\varphi \in [-\pi, \pi]$ cells initially oriented along directions $\theta - \varphi$ or $\theta + \varphi$ may randomly turn into the direction θ . Similarly, cells of initial orientation θ might turn away. Summing the cumulative effect for all turn angles $\varphi \in [-\pi, \pi]$ leads to a net rate of change of the cell density given by

$$\frac{\partial C(\theta, t)}{\partial t} = \int_0^\pi \alpha(\varphi) \{C(\theta + \varphi, t) - 2C(\theta, t) + C(\theta - \varphi, t)\} d\varphi. \quad (1)$$

Equation (1) is an approximation based on motion of the cells in discrete steps which does not take into account a distribution of waiting times.

Expanding terms in the integral in a Taylor series about θ , and assuming that $\alpha(\varphi)$ is fairly sharply peaked about $\varphi = 0$, we find that the leading term approximation to the above is

$$\frac{\partial C}{\partial t} = \mu \frac{\partial^2 C}{\partial \theta^2}, \quad (2)$$

where

$$\mu = \int_0^\pi \alpha(\varphi) \varphi^2 d\varphi. \quad (3)$$

Thus, individual randomness in reorientation leads to population behavior akin to diffusion in the variable θ . Unlike Gail and Boone (1970) this result reflects "random walk" of fibroblasts in orientation, not in space. A similar term occurs in a model for orientations of tips of branches in a growing network (Edelstein-Keshet and Ermentrout 1989)

Now consider the likelihood that a single cell at angle θ contacts and aligns with any other cell. This likelihood depends not only on the number (or more accurately density) of other cells present, but also on the orientations of these cells. In particular, if $C(\theta', t)$ is the density of cells whose direction is θ' , the probability that the "test" cell aligns and sticks to any one of these is

$$\beta K(\theta - \theta') C(\theta', t),$$

$(\theta - \theta')$ being the relative contact angle. Summing over the density of cells at all possible orientations leads to

$$\beta \int_{-\pi}^\pi K(\theta - \theta') C(\theta', t) d\theta'.$$

But this is the probability that a *single* cell is diverted away from angle θ . The net effect on the entire density of cells at angle θ is thus

$$\frac{\partial C}{\partial t}(\theta, t) = \beta C(\theta, t) \int_{-\pi}^\pi K(\theta - \theta') C(\theta', t) d\theta' \equiv -\beta C K * C. \quad (4)$$

The $*$ notation will hereafter be adopted for the above convolution integral.

Erickson (1978) observed pairs of cells and plotted the number of contacts which resulted in lining up of the contacting cell as a function of the contact angle (see Fig. 4 in her paper). Her histogram can be interpreted as defining an angle-dependent contact response function from which we infer the following property of $K(\theta)$: The probability of alignment decreases as the relative angle between contacting cells increases. Beyond some critical angle a , cells do not align (i.e., K is positive and nonincreasing for $0 < \theta < a$). To this we add an assumption that clockwise and anticlockwise turns are equally probable (i.e. K is symmetric about zero, which means that positive and negative angles are equivalent). Thus,

$$K(\theta) = \begin{cases} f(\theta) & 0 \leq \theta \leq a, \\ 0 & a \leq \theta < \frac{\pi}{2}, \end{cases} \quad (5a)$$

and

$$K(-\theta) = K(\theta), \quad -\pi \leq \theta \leq \pi. \quad (5b)$$

About $f(\theta)$ we assume only that it is positive and nonincreasing. For greatest generality we separately treat two possibilities: (a) cells align only head-to-head

and only when the angle of contact is acute; (b) cells align head-to-head for acute contact angle θ or head-to-tail for contact at an obtuse angle $180^\circ - \theta$ with equal probability. These assumptions would, respectively, imply that

$$(a) \quad K = K_s \text{ has a single hump on } [0, \pi] \text{ and} \\ K_s = 0 \quad a < \theta < \pi, \quad -a > \theta > -\pi, \quad (5c)$$

$$(b) \quad K = K_d \text{ is double humped on } [0, \pi] \text{ and} \\ K_d(\theta) = K_d(\pi - \theta) = K_d(-\pi + \theta). \quad (5d)$$

(The subscripts s, d respectively signify single and double humped kernels.) We further normalize K by requiring that

$$\int_{-\pi}^{\pi} K(\theta) d\theta = 1. \quad (5e)$$

It is important to emphasize that as long as $f(\theta)$ is nonincreasing on $0 \leq \theta \leq a$ its exact shape is of no consequence as far as conclusions of our models. For reasons of convenience, numerical results were obtained using the two example cases

$$(1) \quad f_1(\theta) = c_1 \cos\left(\frac{\pi\theta}{2a}\right), \quad (6)$$

$$(2) \quad f_2(\theta) = c_2. \quad (7)$$

See Fig. 2. However, the essential predictions apply to *any nonincreasing function* f . It is the symmetry properties of K and, more particularly, the dichotomy between single and double humped kernels that determine the behavior of the system. We shall see later in the analysis that stability results depend on the Fourier transform of the contact response $\hat{K}(k)$ and more precisely on the quantity $\hat{K}(1 - \hat{K})$. A tabulation of representative choices of $K(\theta)$ and corresponding formulae for $\hat{K}(k)$ are given in Table 1 in the appendix where we also show that double-humped kernels have transforms that are $(1 + \cos k\pi)$ multiples of their single-humped counterparts. The significance of this is that zero crossings ($\hat{K}_d(k) = 0$) occur for all odd integers k in double-humped kernels.

4. Modelling strategy

To expose the essential aspects of pattern formation we used the following strategy in simplifying the problem for the purpose of analytic results. First, we omit the details of spatial density variations in favor of simpler equations, based on the independent variables θ and t . This means that we describe relative numbers of cells at different orientations, but do not concern ourselves with the spatial positions of these cells. Analytic results are then complemented by cellular automata simulations which explore the full spatial behavior.

Second, we separately consider three distinct subproblems, each one representative of a different developmental stage or level of complexity. These are (1) interactions at the level of lamellipodia and cell bodies; (2) interactions between free and bound cells; and (3) interactions between clumps of cells. Subproblem (3) will be considered separately (Ermentrout and Edelstein-Keshet 1990) since it uses different mathematical techniques. In subproblem (2) we further consider three limiting cases in which free cells interact only with other free cells,

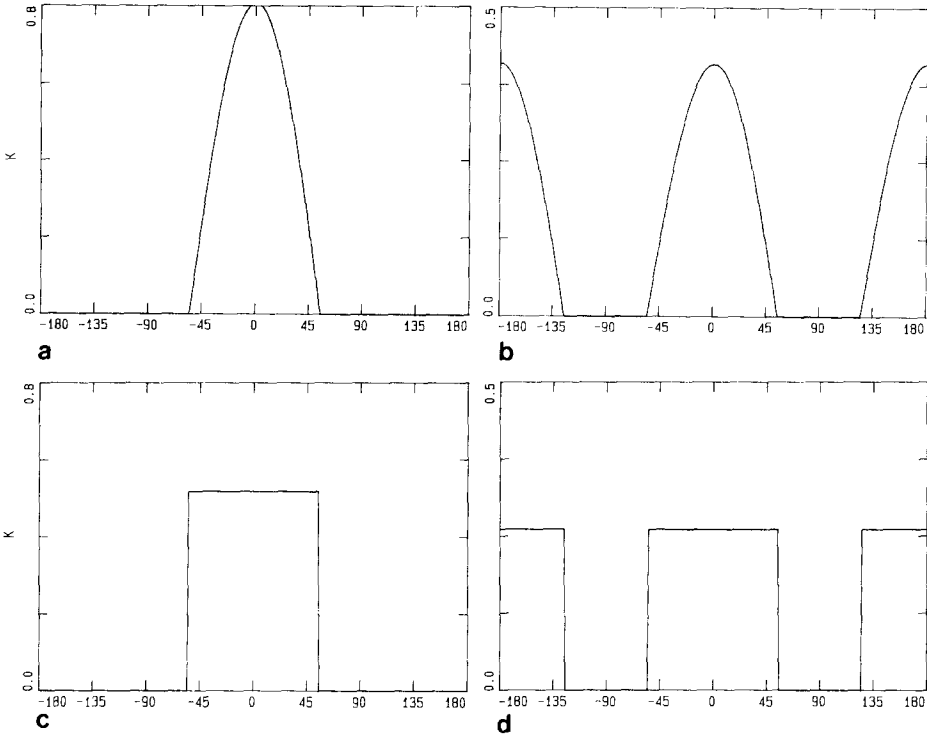


Fig. 2a–d. Shapes of simple angle-dependent kernels mimicking experimental observations. The vertical axis represents probability that contact leads to reorientation and the horizontal axis is the angle between contacting cells. Shown are: **a** K_{1s} ; **b** K_{1d} ; **c** K_{2s} ; **d** K_{2d} (see Table 1). In these graphs the critical angle beyond which cells do not reorient is $\alpha = 55^\circ$

only with bound cells, or with both. Aside from mathematical simplification, this subdivision serves a dual purpose. For one thing, it allows us to place the problem of fibroblasts into a slightly broader context of populations with interacting members. More important, it permits us to pinpoint at what level of complexity the interactions responsible for pattern formation reside.

A third simplification is our treatment of the mass-conserved problem, rather than the problem which explicitly incorporates cell division into the equations. Indeed, later we treat the mass M as a slowly varying parameter. We chose this tactic for the following reasons: (a) Pattern formation is known to occur even in fibroblast cultures which are not actively dividing, provided the density (or total mass) is sufficiently great. (b) When a fibroblast divides it first rounds-up and loses its original orientation. The orientation of the daughters is thus not simply correlated to that of the parent. Thus while cell division increases the total mass, it does so randomly with respect to angles of orientation. This can be modelled explicitly but does not contribute greatly to clarity or intuition. (c) We find that the total mass M can be most conveniently considered as a slowly varying parameter of the system because onset of pattern formation can be explained as a bifurcation which occurs as M exceeds some threshold value.

Thus, while each of our simplifications contribute to mathematical tractability, together, the dissection of the problem into several component parts helps to

reveal the inner workings more effectively than undertaking analysis of a complicated model for the whole phenomenon.

5. Model for lamellipodium/cell-body contacts

Our first model focuses at the level of the components of a cell, namely its reactive leading edge, and its passive body. We consider the angular distributions of the cell bodies and of their lamellipodia. Let $B(\theta, t)$ be the density of cell bodies whose axis of orientation is θ and $L(\theta, t)$ the density of lamellipodia whose direction of motion is θ at time t . (See methods of Dunn and Brown 1987.) The orientation of the body and the direction of motion of its lamellipodium need not always be the same because it takes some time for the orientation of a cell to ooze into the direction in which it is being pulled. Only when cells are in a parallel array are all cell bodies and lamellipodia exactly aligned.

Our model borrows certain notions from the work on branching networks previously cited. Lamellipodia are viewed as the moving particles which can reorient both randomly and through contact. On the other hand, cell bodies are the “tracks” of these particles, in the sense that they are continually “deposited” along directions in which lamellipodia are moving, and lost (due to retraction) from other directions. Cell bodies cannot themselves reorient, but they do cause lamellipodia to reorient, i.e. to disappear from one angle and reappear at some other.

This conceptual framework is conveyed by the equations:

$$\text{Cell bodies} \quad \partial B(\theta, t)/\partial t = vL - \gamma B, \quad (8a)$$

$$\text{Lamellipodia} \quad \partial L(\theta, t)/\partial t = \mu \partial^2 L/\partial \theta^2 - \beta LK * B + \beta BK * L. \quad (8b)$$

The two convolution terms in Eq. (8b) represent lamellipodia reorienting due to contact with cell bodies. The first of these depicts lamellipodia at angle θ being turned via contact with cell bodies at other angles $\varphi \in (-\pi, \pi)$. The second term represents the fact that cell bodies oriented at angle θ can attract lamellipodia whose orientations are initially different from θ . In the equation for cell bodies, vL is the rate that cell-body material is deposited in the track of a moving lamellipodium, and $-\gamma B$ is the “loss” of this material due to retraction where adhesion is broken. The correspondence $(B, L) \rightarrow (q, n)$ leads to equations similar to the branching network model (23a,b) in Edelstein-Keshet and Ermentrout (1989).

One can define a quantity (“total mass”) which is conserved by the dynamics of Eqs. (8). If the relative masses of the cell body and the lamellipodium are δ , and $1 - \delta$ then the total mass,

$$M = \frac{1}{2\pi} \int_{-\pi}^{\pi} \delta B + (1 - \delta)L \, d\theta, \quad (9)$$

is conserved provided that

$$\frac{v}{\gamma} \int_{-\pi}^{\pi} L \, d\theta = \int_{-\pi}^{\pi} B \, d\theta. \quad (10)$$

This means that mass is redistributed as cells reorient but is not created or destroyed.

Homogeneous steady states of Eqs. (8), i.e., populations (\bar{B}, \bar{L}) in which all orientations are equally represented, satisfy

$$v\bar{L} - \gamma\bar{B} = 0, \quad (11)$$

i.e.

$$\bar{L} = \gamma\bar{B}/v, \quad \bar{B} = M/[\delta + \gamma(1 - \delta)/v]. \quad (12)$$

This is a continuum of steady states lying along a straight line with M a parameter. For a fixed initial mass, one point on this line is an attainable steady state. If this steady state is stable, the population would persist in a density ratio of γ/v lamellipodia to cell bodies and no angle or orientation would be favored, in short no alignment of cells would occur. However, if noise can disrupt such a state, i.e. the steady state is unstable, this situation might change to one where some angles are favored. To investigate this possibility we consider perturbations of the form

$$\begin{bmatrix} B(\theta, t) \\ L(\theta, t) \end{bmatrix} = \begin{bmatrix} \bar{B} \\ \bar{L} \end{bmatrix} + \begin{bmatrix} B_0 \\ L_0 \end{bmatrix} e^{ik\theta} e^{\lambda t}. \quad (13)$$

Here B_0, L_0 , the perturbation amplitudes, are small and k , the wavenumber of the perturbation, is an integer since boundaries are periodic.

By methods of Edelstein-Keshet and Ermentrout (1989) the Jacobian of the system of Eqs. (8) is

$$J = \begin{bmatrix} -\gamma & v \\ \beta\bar{L}(1 - \hat{K}) & -\mu k^2 - \beta\bar{B}(1 - \hat{K}) \end{bmatrix}, \quad (14)$$

where \hat{K} is the Fourier transform of the kernel K and k is as above. (K has been normalized, and so $\hat{K}(0) = 1$.) We also define

$$J_0 = \begin{bmatrix} -\gamma & v \\ 0 & 0 \end{bmatrix}. \quad (15)$$

Then J_0 governs perturbations which are angle-independent. We examine whether the homogeneous steady state could be stable to homogeneous but unstable to angle-dependent perturbations.

From the above definitions we find that $\text{Tr}(J_0) = -\gamma$, $\text{Det}(J_0) = 0$, and

$$\text{Det}(J) = \gamma\mu k^2 + \beta(\gamma\bar{B} - v\bar{L})(1 - \hat{K}) = \gamma\mu k^2. \quad (16)$$

We thus find that $\text{Tr}(J_0) < 0$, $\text{Det}(J_0) = 0$, and $\text{Det}(J) > 0$ for all k . This implies stability of the steady state to all perturbations of the form (13) so that pattern formation could not occur through a bifurcation from the uniform steady state. Numerical experiments (not shown here) reveal that the uniform steady state is established from arbitrary initial densities, i.e. is globally stable. We must conclude that an explanation of parallel orientations does not reside at the level of cell-body/lamellipodia contact responses. Some higher level of interactions must then be responsible.

To understand this from an intuitive point of view, consider what happens in a group of cells when noise momentarily causes one direction to be favored. Even if some alignment occurs, the continual random reorientation of lamellipodia will disrupt the pattern. There is no mechanism to overcome this scrambling process, and so parallel orientations cannot be maintained. The model thus reveals that an essential ingredient of the pattern forming mechanism is a step which overcomes random reorientation. We will see below that adhesion of cells

and formation of multicellular complexes which prevent some cells from reorienting provides this step.

6. Interactions of free cells with bound cells

In this section we treat interactions at the level of individual cells, and define $C(\theta, t)$ and $P(\theta, t)$ as densities of free and of bound cells, respectively. Indirectly, the magnitude of $P(\theta, t)$ is related to the total size of a parallel array at that angle. However, since spatial properties are not considered here, only the following functional differences between C and P type cells are assumed: (1) Free cells reorient randomly but bound cells do not. (2) Contact-mediated reorientation can occur when two cells contact; if both contacting cells are initially free, either one of them determines the final orientation with equal probability. In contact between a free cell and a bound cell, the free cell always reorients. (3) All bound cells can become free cells at some fixed unbinding rate γ .

A set of equations depicting these interactions is

$$\text{Bound cells} \quad \frac{\partial P}{\partial t}(\theta, t) = \beta_1 CK * C + \beta_2 PK * C - \gamma P, \quad (17a)$$

$$\text{Free cells} \quad \frac{\partial C}{\partial t}(\theta, t) = \mu \frac{\partial^2 C}{\partial \theta^2} - \beta_1 CK * C - \beta_2 CK * P + \gamma P. \quad (17b)$$

Convolution terms in these equations have the following meanings: In Eq. (17a) $K * C$ represents the rate at which free cells at arbitrary angles contact, align, and bind to other free cells at angle θ , $C(\theta)K * C$, and to bound cells at angle θ , $P(\theta)K * C$. In Eq. (17b) $CK * C$ and $CK * P$ are rates that free cells initially oriented at angle θ are removed through binding to other cells, free and bound, respectively. In Eqs. (17) we have assumed an identical reorientation kernel K for contacts of type $C-C$ as for contacts of type $C-P$. However, we permit different weightings β_1, β_2 in the relative contributions of these interactions. (See the three cases described below.)

It is readily seen that the total mass of this system, defined by

$$M = \frac{1}{2\pi} \int_{-\pi}^{\pi} [C(\theta) + P(\theta)] d\theta, \quad (18)$$

is conserved. (Cells are exchanged between two pools but not added or lost.) We later see that steady states and stability results depend on the dimensionless ratio $\beta M/\gamma$ (where β is related to β_1).

To analyze this model we consider three subcases, two of which are simplified versions of the above. Treating the model in these three steps reveals how each of the interactions contribute to the stability and pattern formation process. In each case we discuss properties of a uniform steady state \bar{P}, \bar{C} and its stability to perturbations of the form

$$\begin{bmatrix} P(\theta, t) \\ C(\theta, t) \end{bmatrix} = \begin{bmatrix} \bar{P} \\ \bar{C} \end{bmatrix} + \begin{bmatrix} P_0 \\ C_0 \end{bmatrix} e^{ik\theta} e^{\lambda t}, \quad (19)$$

where P_0, C_0 are small amplitudes, k is the wavenumber and λ the growth rate of the perturbation.

Case 1. Free cells bind only to free cells ($\beta_1 = \beta, \beta_2 = 0$).

In this case $C(\theta, t)$ and $P(\theta, t)$ denote free and paired cells oriented at angle θ . (Note that by definition P is twice the density of pairs.) Setting $\beta_1 = \beta$ and $\beta_2 = 0$ in Eqs. (17) we find that the interactions between paired cells and free cells are described by the equations:

$$\frac{\partial P}{\partial t} = \beta CK * C - \gamma P, \quad (20a)$$

$$\frac{\partial C}{\partial t} = \mu \frac{\partial^2 C}{\partial \theta^2} - \beta CK * C + \gamma P, \quad (20b)$$

with μ, K as before. A straightforward analysis reveals the following results: (1) The total mass of the system, defined by Eq. (18), is conserved. (2) A single positive θ -independent steady state of Eqs. (20a,b) satisfies

$$\bar{P}/\bar{C} = \beta\bar{C}/\gamma, \quad M = \bar{P} + \bar{C}. \quad (21)$$

(3) This steady state is stable to all perturbations, both uniform and nonuniform. (See the appendix.) These results indicate that if cells are permitted to associate in pairs, but not to form larger clusters there will be a stable combination of free and paired cells at all possible orientations and no preferred directions of orientation will spontaneously arise. Thus pairing is not sufficiently cohesive a force to cause accentuation of parallel orientations.

Case 2. Free cells interact only with bound cells ($\beta_1 = 0, \beta_2 = \beta$).

In this case, $P(\theta, t)$ denotes cells bound in multicellular groups, and we assume that some cell clusters are initially present:

$$\frac{\partial P}{\partial t} = \beta PK * C - \gamma P, \quad (22a)$$

$$\frac{\partial C}{\partial t} = \mu \frac{\partial^2 C}{\partial \theta^2} - \beta CK * P + \gamma P. \quad (22b)$$

From these equations it follows that (1) the total mass of the system, defined by Eq. (18), is constant. (2) For a fixed mass M the model has a single steady state

$$\bar{C} = \gamma/\beta, \quad M = \bar{P} + \bar{C}. \quad (23)$$

In the PC -plane as M varies, the steady state value traces out a line which remains in the first quadrant, i.e. has biological relevance provided $M\beta/\gamma > 1$. (3) This steady state is stable to uniform θ -independent perturbations but could be destabilized by nonuniform perturbations of wavenumber k provided $\hat{K}(k)$ satisfies

$$\hat{K}(\hat{K} - 1) < 0. \quad (24)$$

(See the appendix for details and the solid curves in Fig. 3 for plots of this expression as a function of k .) For case 2 we observe that instability depends only on the Fourier transform of K , and not on other parameters of the system. As we shall see below, this artifact disappears when the full interactions of free and bound cells are considered (case 3).

Because the inequality (24), or equivalently $0 < \hat{K} < 1$ can be satisfied by an infinite set of integer wavenumbers k , we conclude that instability will occur, but cannot use linear theory to make any prediction about which wavelength will be

accentuated as the uniform steady state is destabilized. We infer that in the limit of no cell pairing (i.e. no interactions between free cells) the system is unstable to many perturbations irrespective of parameter settings, and go on to determine how such interactions change this conclusion.

Case 3. Free cells interact with all other cells ($\beta_1 = \beta_2 = \beta$).

We now analyze the full set of Eqs. (17a,b) taking equal β 's. These equations have a single positive steady state

$$\frac{\bar{P}}{\bar{C}} = \frac{\beta M}{\gamma}, \quad M = \bar{P} + \bar{C}, \quad (25)$$

which is stable to uniform (θ -independent) perturbations. After onerous algebra (see the appendix for details) we find that this steady state can be destabilized by perturbations of the form (19) provided

$$Ak^2 < \hat{K}(k)(1 - \hat{K}(k)), \quad (26)$$

where

$$A = \frac{\mu}{\gamma} \left(\frac{\gamma}{\beta M} \right)^2 \quad (27)$$

is a quantity which depends on the parameters of the problem. In particular, A depends on the dimensionless mass ratio $\gamma/\beta M$ which is, by (25), identical with the ratio of free to bound cells at steady state. Further, A depends on μ/γ which depicts the extent of angular spread in a population of free cells during the half life of a bound cell. Thus, unlike the previous cases, here stability depends on parameters governing the biological interactions.

Before interpreting the stability condition (26) we discuss the behavior of the transform $\hat{K}(k)$. Several examples of typical kernels and their Fourier transforms are given in the appendix. It transpires, however, that the essential features of such transforms depend largely on symmetry properties (i.e. whether a single- or a double-humped kernel is assumed) and not on the choice of functional representation on $0 \leq \theta < a$, beyond the fact that $f(\theta)$ is nonincreasing. In the appendix we show that if $K_s(\theta) = K_d(\theta) = f(\theta)$ on $0 \leq \theta < a$ where $f(\theta)$ is nonincreasing, $a < \pi/2$, and K_s , K_d are single- and double-humped kernels then

$$(a) \quad \hat{K}_d(k) = \frac{1}{2} \hat{K}_s(k)(1 + \cos k\pi), \quad (28a)$$

$$(b) \quad 0 < \hat{K}_d(2) < 1, \quad 0 < \hat{K}_s(1) < 1. \quad (28b)$$

Thus, double-humped kernels have Fourier transforms which vanish for all odd wavenumbers $k = 1, 3, 5, \dots$. Further, the first integer value of the wavenumber k for which $\hat{K}(k)(1 - \hat{K}(k))$ is positive is $k = 2$ for double-humped kernels and $k = 1$ for single-humped kernels.

Returning to the stability condition (26) we plot expressions of the form $y = \hat{K}(k)(1 - \hat{K}(k))$ as a function of k and compare to parabolas $y = Ak^2$. By (26) the parabola must be lower than the other function at some integer value of k for instability to be possible at that wavenumber. Figure 3a-d shows the relationship between these curves for the kernels used as examples in Table 1 of the appendix. Since $\hat{K}(1 - \hat{K}) < 0.25$ and $Ak^2 > 0$, only the range $1 < y < 0.25$ is of interest. The graphs of $\hat{K}(1 - \hat{K})$ generally have a series of peaks of oscillating and slowly decreasing heights. Here only the first few such peaks will prove to be important.

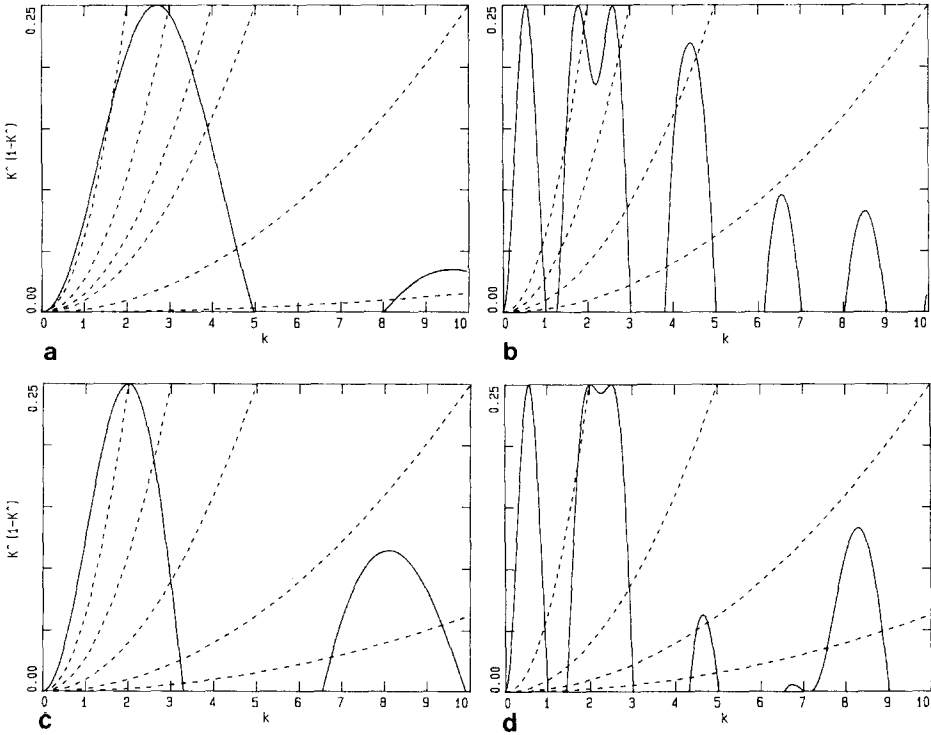


Fig. 3a-d. The expression $y = \hat{K}(k)(1 - \hat{K}(k))$ is shown (solid lines) as a function of the wavenumber k for \hat{K} the Fourier transform of each of the four kernels in Fig. 2: **a** K_{1s} ; **b** K_{1d} ; **c** K_{2s} ; **d** K_{2d} . Superimposed is a set of parabolas $y = Ak^2$ (dashed lines). For a given parabola, $A = 0.25/k_0^2$ where k_0 is the intercept with the top horizontal axis. Pattern formation can only be initiated by a disturbance whose wave number k is an integer satisfying $Ak^2 < \hat{K}(1 - \hat{K})$ where $A = (\mu/\gamma)(\gamma/\beta M)^2$ depends on biological parameters. The sequence of parabolas from left to right could be generated by increasing the total mass of cells, M given that other parameters are constant. For double-humped kernels (right-hand side) $k = 2$ is the first integer wavenumber for which pattern formation can occur, and all odd wavenumbers are excluded. For single-humped kernels (left-hand side) $k = 1$ is the first such wavenumber. See text for further details

By the general properties mentioned above, the graph of $\hat{K}_d(1 - \hat{K}_d)$ where K_d is double humped has zero crossings for $k = 1, 3, 5, \dots$, so that the inequality (26) can never be satisfied for odd k . Thus $k = 2$ is the first wavenumber for which the right-hand side of (26) is positive and thus for which the inequality (26) can be satisfied. Consider the bifurcation phenomenon that occurs as the quantity A decreases from some initially high value: At first, the parabola $y = Ak^2$ might be so steep that it fails to satisfy (26) for any integer. As A decreases, so does the steepness of the parabola. For A suitably small (second and first members of the sequence in Fig. 3b,d), the parabola dips below the other graph at the value $k = 2$. At this point $k = 2$ becomes the first and the only destabilizing wavenumber, i.e. a perturbation of the form $e^{2i\theta}$ would grow. The steady state loses stability and two orientations, 180° apart are accentuated in the cell population, so that cells are mostly parallel to each other, some facing one

way and some facing the other way. The axis of this array, θ^* , is random: in the model, it depends on the initial disturbance that disrupted the steady state.

In the case of single-humped kernels, the first wavenumber at which (26) can be satisfied (for sufficiently small values of A) is $k = 1$. (See, for example, Fig. 3a,c.) Thus, in the bifurcation we have just discussed the steady state destabilizes to a patterned state in which *one* peak predominates in the distribution of orientations. This means that all the cells would tend to align in parallel facing the same direction, not back to front as before.

A point to be emphasized here is the fact that the quantity A in (26), (27) depends on parameters governing biological properties of the system. Thus, changing any one of the parameters μ , γ , M , or β affects stability (unlike case 2). For example, during a normal course of development, cell division causes the total mass M to increase. This is synonymous with decreasing A , thus leading spontaneously to a bifurcation of the sort described above, i.e. to formation of parallel arrays. Other biological possibilities include decrease in the random reorientation rate μ , decrease in the rate of shedding of cells from clumps, γ , or increase in the probability β that contact of cells leads to binding. Any one of these effects in isolation could create the above bifurcation. If, on the other hand, parameters are fixed so that A is quite small, we find that many wavenumbers potentially satisfy (26) (e.g. $k = 4$ for the third and fourth parabolas in Fig. 3b and $k = 8$ for the last parabola in Fig. 3d). In the case of double-humped kernels, odd wavenumbers are excluded from patterned states. However, linear theory cannot then predict what happens when several competing wavelengths interact since the dynamics are nonlinear except close to steady state.

In the three limiting cases discussed above, stability characteristics range from unconditional stability (case 1) to instability for a multitude of wavelengths (case 2). Case 3, the most realistic, is perched midrange with stability conditional on a balance between parameters. In case 3 there is competition between opposing forces. On the one hand, the tendency to aggregate stabilizes certain directions, since clumps preserve a fixed orientation. On the other hand, tendency to leave clusters and random reorientation causes directional bias to be erased. Thus dependence on parameters becomes fairly clear: If cells are not very cohesive, (i.e. γ the rate of shedding is large) or μ , the rate of reorientation is large, the tendency for scrambling will be stronger than the tendency to accentuate any particular direction, so that no pattern would be amplified. Further, if \bar{P}/\bar{C} , the ratio of bound cells to free cells at equilibrium (which incidentally, is the same as $\beta M/\gamma$ in case 3) is not large enough, the number of contacts between free and bound cells will be too small for efficient recruitment of cells into clumps. This explains some aspects of the condition for instability (26).

We can also explain the aspects of cases 1 and 2 which lead to extremes of stability and instability. First, in case 1, pairs of cells are fixed in orientation, but they do not recruit other cells and so no mechanism for amplifying a given orientation is present. In case 2 the opposite situation occurs since cells interact *only* with clumps. A clump that is bigger (i.e. a direction that has a greater density of bound cells) can compete more effectively for recruits. Thus any set of directions that have initial advantage could potentially grow, meaning that the steady state can be destabilized by many possible forms of noise, or many wavenumbers.

There is an interesting distinction between cases 2 and 3. The analysis reveals that formation of pairs (i.e. clusters newly generated from pairs of free cells) has a *stabilizing* effect (since the condition for instability is more stringent in case 3

than in case 2). This makes sense since, in recruiting free cells, new clusters compete with more well established ones. Because new clusters form at all possible directions, this competition tends to scramble the possible dominance of a given orientation or set of orientations. As previously discussed, the possibility of maintaining and amplifying certain orientations then depends on parameters governing the cohesion versus the random turning of cells.

To study the dynamics of cases 1–3 we used two approaches. Here we discuss numerical analysis of Eqs. (17). (In Sect. 7 we describe a cellular automaton approach.) The variables were discretized on a grid of 20 points ($\Delta\theta = 360^\circ/20 = 18^\circ = 0.314$ radians). We used a finite difference scheme with $\Delta t = 0.01$ and forward differencing for 10 000–30 000 iterations. Typical kernels (see Table 1 of appendix) were used in a given simulation. In the results shown, the critical angle $a = 55^\circ$ and other parameter values are fixed at $\gamma = \mu = \beta = 0.3$. We used a variety of initial densities $P = P_0 + p'(\theta, t)$, $C = C_0 + c'(\theta, t)$ (p' , c' random deviations with magnitudes roughly 10% of P_0 , C_0 respectively) and so we were able to vary the total mass $M \approx P_0 + C_0$.

Results are as follows: (1) Initially, densities of free and bound cells are seen to adjust so that the average ratio P/C approaches that predicted by the uniform steady state. Only then does further development occur. (2) Predictions of the analysis matched numerical results: In case 3, as M was increased beyond a threshold level ($M_c \approx 4.0$) a bifurcation of the steady state leading to patterns with two peaks ($k = 2$) appeared (see Fig. 4). (3) In case 1, where only cell pairs occur, pattern formation did not occur for any conditions tested. (The population returned to the uniform steady state.) (4) In case 2, where cells interact only with clumps, the steady state would always be destabilized by random deviations. Patterns in case 2 characteristically took longer to form initially because of competition between many modes. However, they eventually grew faster and acquired sharper peaks than those of case 3. We found that a single mode was eventually selected. For example, as shown in Fig. 5, the mode $k = 2$ grows, a fact which could not be predicted by the linear stability analysis. (5) In case 3, when the total mass exceeded its bifurcation value, several wavelengths were able to grow initially. For example, with $M = 5$ and single-humped kernel $K = K_{2s}$, we see that $k = 1$ and $k = 2$ grow, but $k = 1$ eventually wins (see Fig. 6). With $K = K_{2d}$ and $M = 5$, only the wavelength $k = 2$ can grow.

7. Cellular automata models

The spatial behavior of a population of fibroblasts can be studied using a cellular automata model. We found this approach both computationally convenient and visually striking. While details of this model will be presented in a separate paper, we here outline the salient features. Briefly, a rectangular region is subdivided into a grid of $n \times m$ squares, each of which can be either empty, or occupied by a free or a bound cell. For convenience, we considered a discrete set of 8 orientations, either $l = 8$ or $l = 16$. Cells, represented by rods, move in the direction to which they point, i.e. along straight line segments. For example, for $l = 8$, a free cell occupying a given square, moves into one of its eight neighboring squares each time step and makes 45° turns. Free cells can undergo reorientation upon contact with other free or bound cells, or randomly, as they move over the grid. Interactions between cells are governed by

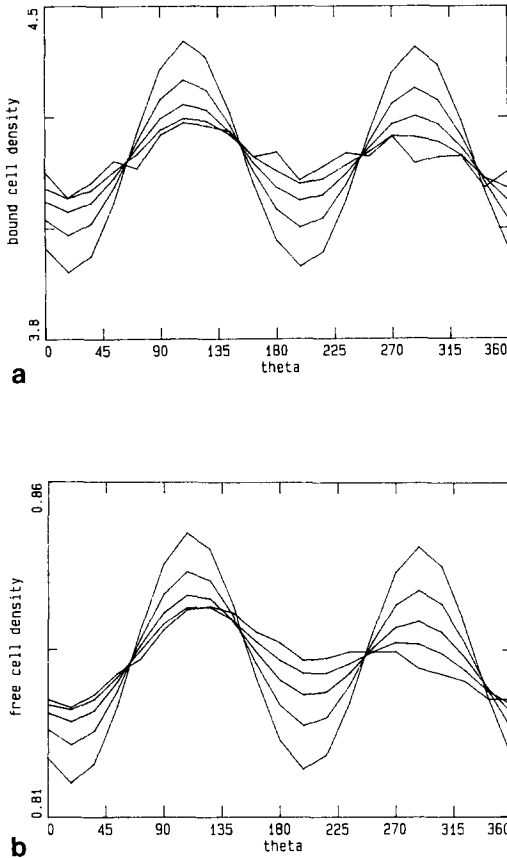


Fig. 4a,b. Formation of structure in a population of free and bound cells with contact and random reorientation. Shown are numerical solutions to Eqs. (17) in the case when free cells interact with both free and bound cells (i.e. case 3 with $\beta_1 = \beta_2 = \beta = 0.3$). The horizontal axis is orientation and the vertical axes are the densities of bound and free cells at a given orientation. Initial densities (not shown) were $P(\theta, t) = 0.5 + p_0(\theta, t)$, $C(\theta, t) = 4.5 + c_0(\theta, t)$ where p_0, c_0 are 10% random noise. The contact-reorientation response used was $K = K_{2,d}$ (see Table 1) with critical angle $a = 55^\circ$. (Thus $\hat{K}(2)(1 - \hat{K}(2)) \approx 0.25$; see Fig. 3d.) Other parameters are $\gamma = \mu = 0.3$. The solutions were found for 20 000 iterations, with plots at increments of 4000 iterations. In this example, the total mass $M = P + C \approx 5.0$ exceeds the critical value $M_c = 2(\gamma/\beta)[\hat{K}(2)(1 - \hat{K}(2))]^{-1/2}(\mu/\gamma)^{1/2} \approx 4.0$ at which $k = 2$ becomes unstable. Thus the density distributions develop two peaks, so that two orientations, 180° apart are accentuated in the population. (In this case, at $\theta^* = 110^\circ$ and at $180^\circ + \theta^*$.) Note scales on a bound cells and b free cells indicate that most cells are bound

angle-dependent contact responses in an exact discrete analogue of case 3, Sect. 6. Here, however, the spatial as well as angular distributions can be seen.

The initial configuration is that of a dense culture of free cells, with a random distribution of orientations. There is a fairly rapid coagulation into clusters of bound cells, but for a long time no apparent order exists in orientations of these clumps. On a relatively fast PC, a simulation with 500–1500 cells can be followed visually much like the time-lapsed photography of motions of real cultures, and gives one a keen appreciation of the dynamics involved. Since adjustable parameters allow us to tune the rate of shedding of cells, the initial mass, and other factors, we can study how such properties affect the appearance and evolution of the population including geometry (Fig. 7) and angular density (Fig. 8).

To focus on interactions devoid of external cues, we chose periodic boundary conditions, “cells moving on the surface of a torus”. Thus the orientations of the arrays cannot be influenced by external biases such as boundaries or contact with other tissues. Figure 7 shows typical development in the cellular automaton. After some lengthy exchange of “cells”, organization into a few clusters occurs (see Fig. 7b). This stage is analogous to the stage shown in Fig. 1b, in which a collection of parallel arrays coexist. However, if the process is allowed to continue (and this last stage takes comparatively long), eventually one of the clumps overtakes the others in competing for material, and a single array,

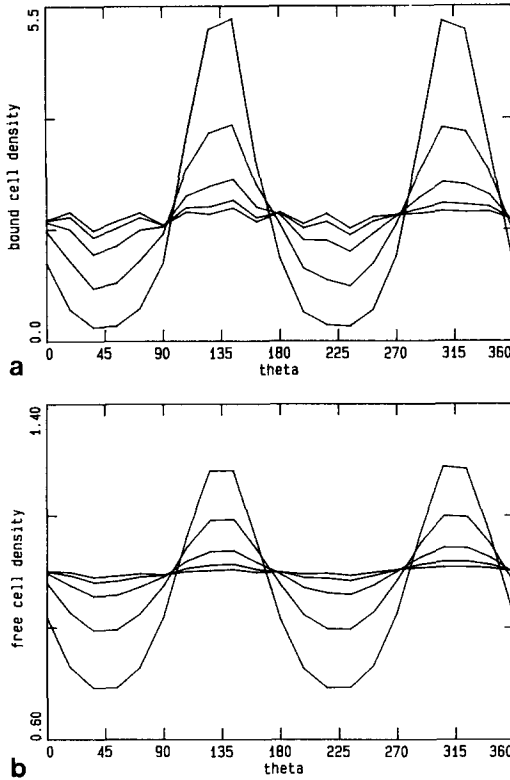


Fig. 5a,b. Numerical simulations of Eqs. (17) with $\beta_1 = 0, \beta_2 = \beta = 0.3$ (case 2), i.e. free cells interact only with bound cells. Initial densities were $P(\theta, t) = 0.1 + p_0(\theta, t), C(\theta, t) = 2.9 + c_0(\theta, t)$, with p_0, c_0 10% random noise as before. All other conditions identical with Fig. 4. Here the values of parameters and total mass are irrelevant for stability of the steady state. Yet, the nonlinear interactions engender the selection of two orientations, as before. Because new clusters of bound cells cannot appear, after initial transient the orientations $\theta^* = 135^\circ, \theta^* + 180^\circ$ grow faster and produce sharper peaks than in case 3 shown in the previous figure

containing cells both parallel and antiparallel will emerge (Figs. 7d, 8). This array is thereafter stable, although it continues to change shape somewhat since cells are still being liberated and captured. The fact that this eventual outcome is attained in the absence of boundary constraints means that the tendency to form a single axis of orientation is an inherent population phenomenon, independent of external organization. This property exhibited by our cellular automation agrees with predictions of the continuum model of Sect. 6. Nübler-Jung (1987) suggested that in a field with two parallel boundaries, the pattern of orientations will simplify into a single parallel array, but we have shown that this property is not dependent on the boundaries. The winning direction is different in different runs using identical parameter values. This stems from the fact that many small tugs and pulls combine to determine the final outcome. If we permit boundaries to exert an effect, we would clearly introduce a bias which would affect the final pattern.

Since the analytical work presented in this paper has dealt only with angular distributions, and has been restricted to simplified versions of the process, the cellular automaton simulations help us to bridge a gap in realism. The results of our simulations confirm the belief that individual cellular interactions, in the absence of long-range gradients, of orienting fibers, or of other environmental cues, can lead to formation of pattern such as the phenomenon of parallel orientation in fibroblast cultures.

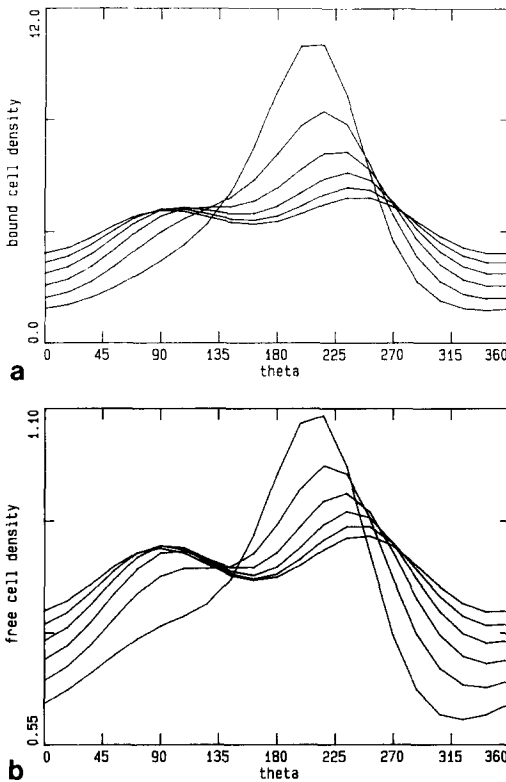


Fig. 6a,b. Simulations of Eqs. (17) with parameter values and initial conditions identical to those in Fig. 4, but with $K = K_{2s}$, i.e. a single-humped contact response (cells reorient and stick only if contact is at an acute angle). From Fig. 3c we find that the parameter settings, which made $k = 2$ unstable, also make $k = 1$ unstable. Both modes grow for some time, but eventually, nonlinear interactions (which cannot be explained on the basis of linear stability analysis) favor the wavenumber $k = 1$. Thus a single orientation, $\theta^* \approx 205^\circ$ is accentuated, i.e. cells tend to face in the same direction at that orientation. Shown are plots starting at 20 000 iterations and evolving towards a single peak at increments of 2000 iterations. For a larger total mass (e.g., $M = 12$), $k = 2$ predominates, and the development is faster, leading to sharper peaks

8. Discussion

Previous theoretical considerations of patterns in fibroblast cultures appear in papers by Elsdale (1972, 1973) and by Elsdale and Wasoff (1976). Their approach is a topological one dealing with the discontinuities observed between neighboring arrays using index theory. (See also Penrose 1965.) The models we have described are aimed at understanding the dynamical process of array formation, at bridging a gap between the behavior of the individual cell and that of the population, but not at understanding spatial structure directly. Thus, our mathematical techniques differ from those of Elsdale and coworkers. (But see Ermentrout and Edelstein-Keshet 1990 for a treatment of interactions between aggregates of cells.)

It is an interesting coincidence that phenomena of parallel alignment occur in numerous disparate systems, including physical and chemical ones. A notable example in three dimensions is that of liquid crystals. (See Priestly et al. 1975 for a good introduction.) An extensive body of physical theory has been developed to account for the orientational distribution of molecules in a variety of liquid crystal types, for local and long-range order, and for phase transitions in response to temperature and applied external fields. Statistical mechanics and thermodynamic methods are predominant tools of the trade, and the arguments revolve around minimization of free energy and/or maximization of entropy associated with the molecular order in an equilibrium state.



Fig. 7a–f. Results of the cellular automata model described in Sect. 7 and analogous to case 3 of the model in Sect. 6. This is a full spatial model, with cells (shown as line segments) moving over a rectangular region, reorienting, and sticking to cells or clumps they contact. (Motion is in the direction opposite the square tails.) There are 16 possible orientations, at 22.5° increments. Shown is the sequence of steps at times **a**; **b** 150; **c** 350; **d** 650; **e** 850; **f** 2000 after the start of the simulation. The cells are initially randomly oriented and gradually develop into parallel arrays which then simplify into the final structure. The simulation incorporated 600 cells on a 40×20 grid with periodic boundaries (cells moving on a torus). Parameters were as follows: probability of sticking on contact = 0 for cells forming a 90° contact angle, 0.2 otherwise. Probability of cell release from a clump per move = 0.1. Probability of random reorientation per free cell per move = 0.1

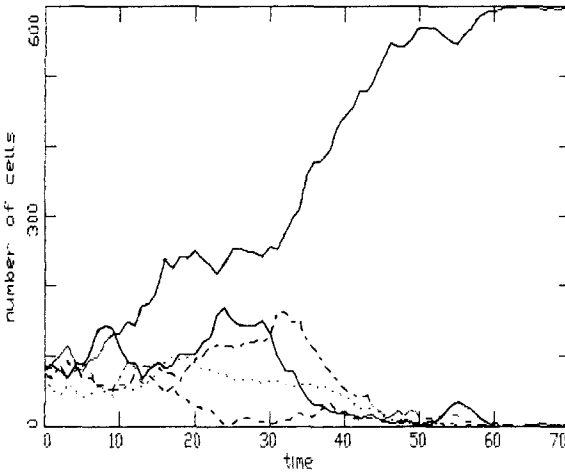


Fig. 8. The number of cells is shown at several orientations as a function of time. (Each time unit is equivalent to 20 steps of the previous figure.) One orientation (that shown in Fig. 7f) eventually wins the competition. For clarity, not all orientations are plotted and data for an angle θ are pooled with that of $\theta + \pi$

Theories accounting for liquid crystal geometry take into account the anisotropic attraction between elongated molecules, as well as steric effects due to impenetrability. Onsager (1949) was among the first to demonstrate that a collection of hard rods, even ones without any mutually attractive interactions, would tend, with increasing density, to favor a parallel conformation. (The observation stems from a trade off between orientational and translational entropy; in the high density limit, the effects of excluded volume which occur if molecules are not aligned overrides the decrease in the orientational entropy.)

Analogies between liquid crystals and parallel cells are appealing but limited. First, specific details of the interactions differ. Perpendicular rods are unstable, but perpendicular cells are not: experiments indicate that contact angles close to 90° fail to induce cell alignment. Second, thermodynamic arguments for liquid crystals are inapplicable to cell biology (see Harrison 1982, 1990). We must not forget that biological systems such as the one here described operate far from thermodynamic equilibrium, and that free energy or entropy arguments do not apply to cellular geometry. In all aspects of their behavior, cells expend energy—they are not impenetrable rods whether inert or attractive—but rather miniature machines which shape and affect the environment and each other in a dynamic way.

We list here some of the predictions and conclusions of our analysis. In interpreting such predictions, one must take into account the assumptions on which our models are based and the fact that they are simplified and abstracted versions of the real situation.

(1) Some form of cohesion which restricts free motion is essential for the formation of parallel arrays. In the absence of formation of multicellular aggregates, parallel orientations would not spontaneously arise, as shown in Sect. 5. In the fibroblast example, cohesion takes the form of cell-surface chemistry that causes cells to stick to each other in clumps.

(2) Binding in pairs is not sufficiently cohesive to lead to parallel orientations. Larger multicellular complexes are necessary to promote a given orientation by diminishing the scrambling effect of random cellular reorientation.

(3) The phenomenon is not highly sensitive to details of the contact-response, and depends only on rather broad features of the kernels modelling this

response. The main effects hinge on whether the response of cells contacting at an angle θ is the same as that for $180^\circ - \theta$ or not (i.e. whether the kernel K is single or double humped). If cells do not respond to contacts at obtuse angles, we find clumps in which cells are all facing the same direction. If, on the other hand, obtuse or acute contact angles are equivalent, clumps always contain cells which face back to front.

(4) The alignment of cells is sensitive to parameters governing the system, i.e. to the total mass of cells M , to the rate of adherence, β , the rate of shedding, γ , and the rate of random reorientation, μ . (See Eqs. 26, 27.) The relative magnitudes of the total mass M and the value of γ/β , a ratio of shedding to recruitment of cells by a clump, has several effects. (a) It governs relative proportions of free and bound cells. (b) It governs the tendency to recruit cells into clumps and thus determines whether patterns such as parallel arrays will form. The parameter μ influences only the latter process.

(5) Simulations confirm that a configuration in which all cells are parallel will occur when these interactions are permitted without any other additional assumptions. It is not necessary to assume external organizing effects, global constraints, boundaries, or contact with other tissues to get a single field of parallel orientations (contrary to the implication in Nübler-Jung). However, where effects such as boundaries, gradients, or oriented fibers do exist, the preferred orientation of the final pattern will be influenced or predetermined.

(6) In the models and simulations we studied, the final outcome, one which was attained at the end of a lengthy process of adjustment and readjustment was *always* the formation of a single parallel array. Thus, if in a given biological example a pattern culminates in many coexisting parallel arrays, other effects must be at work. Such effects could include arrestment of the developmental process, permanent adhesion of cells which would halt the exchange and competition between arrays, spatial variation in environmental effects that locally favor certain orientations, or interactions with other substances (e.g., collagen) not explicitly considered here.

Finally, we wish to indicate the range of applicability of models like this one to systems other than those drawn from the biology of cells. As previously mentioned, similar phenomena occur in multicellular organisms at many size scales. Jander and Daumer (1974) describe self-organized foraging columns of termites in which orientation is selected by continual collisions between stray individuals and those in the columns. (Here, cohesion of a group is mediated by chemical trail-following.) Similar phenomena occur in other social insects (Deneubourg and Goss 1989). Swarming and herding behaviors in animal groups have been studied extensively (see Okubo 1986 for review), but a greater emphasis has been placed on spatial density distributions, rather than orientations. In groups or herds the responses and motion of the individual are behaviorally affected by its immediate neighbors. Although the biological mechanisms leading to herding are clearly quite remote from the cell-surface chemistry that governs contacts of fibroblasts, the analogies of contact response are clear. Thus, similar approaches may prove useful in these settings.

As a somewhat more abstract application, one could extend models such as those of Sect. 6 to cases in which θ stands for some other state variable, not necessarily a real orientation (e.g., a political orientation or persuasion). If individuals are indecisive (reorient randomly) but can persuade or be persuaded

by others whose views are similar (not far separated in θ), and if cohesive groups of persuasion form and recruit members, then a rather similar model would apply. This lighthearted example suggests that the mathematical methods used in this paper, namely integro-differential equations, have a wide range of applicability. Models similar to the ones here explored could therefore be useful in areas other than cell biology.

Acknowledgements. During initial stages of this work as a visitor at Duke University, L.E.K. was supported by a National Science Foundation grant DMS-86-01644; in later stages, she was supported by a Natural Sciences and Engineering Research Council of Canada operating grant OGPIN 021. G.B.E. was supported by a National Science Foundation grant DMS-87-01405. We are grateful for comments and discussions with W. Alt, J. L. Deneubourg, L. G. Harrison and V. Calenbuhr.

Appendix

A. Typical kernels and their Fourier transforms

We first show the connection between Fourier transforms of single- and double-humped kernels. For $K(x) = f(x)$ on $0 \leq x \leq a$, define

$$N = \int_0^a f(x) dx,$$

$$I(k) = \int_0^a f(x) \cos kx dx.$$

By symmetry of K about zero, we find that the Fourier transform of a single-humped kernel is

$$\hat{K}_s(k) = I(k)/N.$$

For a double-kernel,

$$\hat{K}_d(k) = \frac{1}{2N} \left(I(k) + \int_{\pi-a}^{\pi} f(\pi-x) \cos kx dx \right).$$

By a simple variable transformation it is seen that the integral above can be rewritten as

$$\cos k\pi \int_0^a f(u) \cos ku du.$$

Thus

$$\hat{K}_d(k) = \frac{I(k)}{2N} (1 + \cos k\pi) = \hat{K}_s(k) \left(\frac{1 + \cos k\pi}{2} \right).$$

Next, we observe that $0 < \hat{K}_s(2) < 1$. To do so, we require that $f(x)$ be nonincreasing and that $a < \pi/2$. The argument that $\hat{K}_s(2) > 0$ involves the sign of the quantity

$$\int_0^a f(x) \cos 2x dx.$$

In case $0 < a < \pi/4$ the integrand is strictly positive and we are done. If however

Table 1

$K(\theta)$	Fourier transform
$K_{1s}(\theta) = \begin{cases} \frac{\pi}{4a} \cos(\pi\theta/2a) & \theta < a \\ 0 & \theta \geq a \end{cases}$	$\hat{K}_{1s}(k) = -\left(\frac{\pi}{2a}\right)^2 \frac{\cos ka}{k^2 - (\pi/2a)^2}$
$K_{1d}(\theta) = \begin{cases} \frac{1}{2}K_{1s}(\theta) & \theta < \frac{\pi}{2} \\ \frac{1}{2}K_{1s}(\theta - \pi) & \theta > \frac{\pi}{2} \end{cases}$	$\hat{K}_{1d}(k) = \frac{1}{2}\hat{K}_{1s}(k)(1 + \cos k\pi)$
$K_{2s}(\theta) = \begin{cases} \frac{1}{2a} & \theta < a \\ 0 & \theta \geq a \end{cases}$	$\hat{K}_{2s}(k) = \frac{\sin ka}{ka}$
$K_{2d}(\theta) = \begin{cases} \frac{1}{2}K_{2s}(\theta) & \theta < \frac{\pi}{2} \\ \frac{1}{2}K_{2s}(\theta - \pi) & \theta > \frac{\pi}{2} \end{cases}$	$\hat{K}_{2d}(k) = \frac{1}{2}\hat{K}_{2s}(k)(1 + \cos k\pi)$

$\pi/4 < a < \pi/2$, split the above into

$$\left(\int_0^{\pi/4} + \int_{\pi/4}^a \right) f(x) \cos 2x \, dx$$

and observe that the second integral, which is negative, is in absolute value smaller than the first.

Table 1 gives two examples each, of single-humped (K_{1s}) and double-humped (K_{1d}) kernels with their Fourier transforms, \hat{K} . The shapes of the kernels are shown in Fig. 2.

B. Stability analysis. Eqs. (17)

To determine stability of the steady states in cases 1–3 of Sect. 6 we examine the trace and determinant of the Jacobian of Eqs. (17) in each of the three cases. For notational convenience we define

$$J = \begin{bmatrix} -\varepsilon & \xi \\ \eta & -\delta \end{bmatrix} \tag{A1}$$

and tabulate the entries $\varepsilon, \eta, \xi, \delta$ in Table 2. We observe that ε and δ are always nonnegative since $\bar{P}/\bar{C} > 0$ and $\bar{P}/\bar{M} > 0$ at the biologically relevant steady states and since $|\hat{K}| < 1$. Thus $\text{Tr}(J) = -(\varepsilon + \delta)$ is negative in each of the three cases. For stability to uniform perturbations and instability to θ -dependent perturbations, it is necessary that $\text{Det}(J) = \varepsilon\delta - \xi\eta$ be nonnegative for $k = 0$ and negative for some integer wavenumber k . Such an integer is then a destabilizing mode.

Calculations of the appropriate expression is trivial in all but the last case, where algebraic simplification is more cumbersome. Defining $Q = \beta\bar{C}(1 + \hat{K})$,

Table 2. Elements in the Jacobian (A1)

	Case 0: $\beta_1 \neq \beta_2 > 0$	Case 1: $\beta_1 = \beta, \beta_2 = 0$	Case 2: $\beta_1 = 0, \beta_2 = \beta$	Case 3: $\beta_1 = \beta_2 = \beta$
Steady state	$\bar{P}/\bar{C} = \beta_1 \bar{C}/(\gamma - \beta_2 C)$	$\bar{P}/\bar{C} = \beta \bar{C}/\gamma$	$1 = \beta \bar{C}/\gamma$	$\bar{P}/\bar{C} = \beta M/\gamma$
ϵ	$\gamma - \beta_2 \bar{C}$	γ	0	$\gamma - \beta \bar{C}$
η	$\gamma - \beta_2 \bar{C} \hat{K}$	γ	$\gamma(1 - \hat{K})$	$\gamma - \beta \bar{C} \hat{K}$
ξ	$\beta_1 \bar{C}(1 + \hat{K}) + \beta_2 \bar{P} \hat{K}$	$\beta \bar{C}(1 + \hat{K})$	$\beta \bar{P} \hat{K}$	$\beta \bar{C}(1 + \hat{K}) + \beta \bar{P} \hat{K}$
δ	$\mu k^2 + \beta_1 \bar{C}(1 + \hat{K}) + \beta_2 \bar{P}$	$\mu k^2 + \beta \bar{C}(1 + \hat{K})$	$\mu k^2 + \beta \bar{P}$	$\mu k^2 + \beta \bar{C}(1 + \hat{K}) + \beta \bar{P}$
Det(J)	$\gamma \mu k^2$	$\gamma \mu k^2$	$-\bar{P} \beta \gamma \hat{K}(1 - \hat{K})$	$\frac{\beta \gamma \bar{C}^2}{\bar{P}} \left[\frac{\mu k^2}{\gamma} - \hat{K}(1 - \hat{K}) \left(\frac{\beta M}{\gamma} \right)^2 \right]$
Instability	Never	Never	Too many wavenumbers (whenever $0 < \hat{K} < 1$)	When $Ak^2 < \hat{K}(1 - \hat{K})$ $A = \frac{\mu}{\gamma} \left(\frac{\gamma}{\beta M} \right)^2$

$S = \beta\bar{P}$, $L = \mu k^2$, we have

$$\begin{aligned} \text{Det } J &= (\gamma - \beta\bar{C})(L + Q + S) - (\gamma - \beta\bar{C}\hat{K})(Q + S\hat{K}) \\ &= (\gamma - \beta\bar{C})L + (\hat{K} - 1)[Q\beta\bar{C} - \gamma S + SQ] \\ &= (\gamma - \beta\bar{C})L + (\hat{K} - 1)[Q\beta(\bar{C} + \bar{P}) - \gamma S] \\ &= (\gamma - \beta\bar{C})L + \beta(\hat{K} - 1)[M\beta\bar{C}(1 + \hat{K}) - \gamma\bar{P}]. \end{aligned} \quad (\text{A2})$$

Using $(\gamma - \beta\bar{C}) = \beta\bar{C}^2/\bar{P}$ and $\gamma\bar{P} = \beta\bar{C}M$ and regrouping terms eventually leads to

$$\text{Det } J = \frac{\beta\gamma\bar{C}^2}{\bar{P}} \left[\frac{\mu k^2}{\gamma} + (\hat{K} - 1)\hat{K} \left(\frac{M\beta}{\gamma} \right)^2 \right]. \quad (\text{A3})$$

References

- Alt, W.: Biased random walk models for chemotaxis and related diffusion approximations. *J. Math. Biol.* **9**, 147–177 (1980)
- Bard, J., Elsdale, T.: Growth regulation in multilayered cultures of human diploid fibroblasts: the roles of contact, movement and matrix production. *Cell Tissue Kinet.* **19**, 141–154 (1986)
- Bard, J. B. L., Hay, E. D.: The behavior of fibroblasts from the developing avian cornea, morphology and movement in situ and in vitro. *J. Cell. Biol.* **67**, 400–418
- Deneubourg, J. L., Goss, L.: Collective patterns and decision-making. *Ethology, Ecology, and Evolution*, **1**, in press (1990)
- Dunn, G. A., Brown, A. F.: A unified approach to analysing cell motility. *J. Cell Sci. Suppl.* **8**, 81–102 (1987)
- Edelstein-Keshet, L., Ermentrout, G. B.: Models for branching networks in two dimensions. *SIAM J. Appl. Math.* **49**, 1136–1157 (1989)
- Elsdale, T.: Pattern formation in fibroblast cultures, an inherently precise morphogenetic process. In Waddington, C. H. (ed.) *Towards a theoretical biology*, vol. 4. Edinburgh: Edinburgh University Press 1972
- Elsdale, T.: The generation and maintenance of parallel arrays in cultures of diploid fibroblasts. In Kulonen, E., Pikkarainen, J. (eds.) *Biology of fibroblast*. New York: Academic Press 1973
- Elsdale, T., Bard, J.: Cellular interactions in mass cultures of human diploid fibroblasts. *Nature* **236**, 152–155 (1972)
- Elsdale, T., Bard, J.: Cellular interactions in morphogenesis of epithelial mesenchymal systems. *J. cell Biol.* **63**, 343–349 (1974)
- Elsdale, T., Wasoff, F.: Fibroblast cultures and dematoglyphics: the topology of two planar patterns. *Wilhelm Roux's Archives* **180**, 121–147 (1976)
- Erickson, C. A.: Analysis of the formation of parallel arrays by BHK cells in vitro. *Exp. Cell Res.* **115**, 303–315 (1978)
- Ermentrout, G. B., Edelstein-Keshet, L.: Winner takes all; interactions of cell aggregates. In preparation (1990)
- Gail, M. H., Boone, C. W.: The locomotion of mouse fibroblasts in tissue culture. *Biophys. J.* **10**, 980–993 (1970)
- Harris, A. K., Stopak, D., Warner, P.: Generation of spatially periodic patterns by a mechanical instability: a mechanical alternative to the Turing model. *J. Embryol. Exp. Morphol.* **80**, 1–20 (1984)
- Harrison, L. G.: An overview of kinetic theory in developmental modeling. In: Subtelny, S., Green, P. B. (eds.) *Developmental order: Its origins and regulation*. New York: Liss 1982
- Harrison, L. G.: *Kinetic theory of living pattern*. Cambridge University Press: to be published
- Jander, R., Daumer, D.: Guide-line and gravity orientation of blind termites foraging in the open (termitidae: *Macrotermes*, *Hospitalitermes*). *Paris: Insectes Sociaux*, **21**, 45–69 (1974)
- Keller, E. F., Segel, L. A.: The initiation of slime mold aggregation viewed as an instability. *J. Theor. Biol.* **26**, 399–415 (1970)

- Lackie, J. M.: Cell movement and cell behavior. Boston: Allen and Unwin 1986
- Murray, J. D., Oster, G. F.: Cell traction models for generating pattern and form in morphogenesis. *J. Math. Biol.* **19**, 265–279 (1984)
- Nübler-Jung, K. Tissue polarity in an insect segment: denticle patterns resemble spontaneously forming fibroblast patterns. *Development* **100**, 171–177 (1987)
- Okubo, A.: Dynamical aspects of animal grouping: swarms, schools flocks, and herds. *Adv. Biophys.* **22**, 1–94 (1986)
- Onsager, L.: The effects of shapes on the interaction of colloidal particles. *Ann. N.Y. Acad. Sci.* **51**, 627 (1949)
- Oster, G. F., Murray, J. D., Harris, A. K.: Mechanical aspects of mesenchymal morphogenesis. *J. Embryol. Exp. Morph.* **78**, 83–125 (1983)
- Priestly, E. B., Wojtowicz, P. J., Sheng, P. (eds.) Introduction to liquid crystals. New York: Plenum Press, 1975
- Penrose, L. S.: Dermatoglyphic topology. *Nature* **205**, 544–546 (1965)
- Shapiro, J. A.: Bacteria as multicellular organisms. *Scientific Am.* June, pp. 82–89 (1988)
- Stopak, D., Harris, A. K.: Connective tissue morphogenesis by fibroblast traction I. Tissue culture observations. *Dev. Biol.* **90**, 383–398 (1982)
- Trinkaus, J. P.: Some thoughts on directional cell movement during morphogenesis. In Bellairs, R., Curtis, A., Dunn, G. (eds.) Cell behavior. Cambridge University Press 1982
- Trinkaus, J. P.: Further thoughts on directional cell movement during morphogenesis. *J. Neurosci. Res.* **13**, 1–19 (1985)